

# Aryl–Fluoride Bond-Forming Reductive Elimination from Nickel(IV) Centers

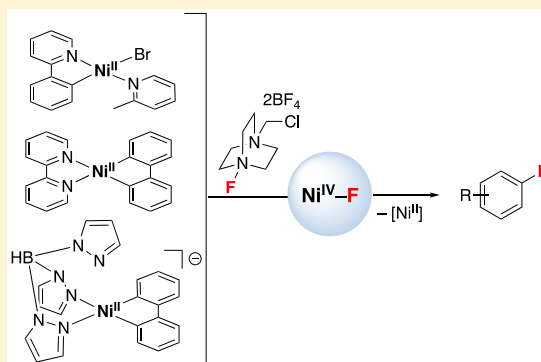
Elizabeth A. Meucci,<sup>†</sup> Alireza Ariafard,<sup>‡</sup> Allan J. Canty,<sup>‡</sup> Jeff W. Kampf,<sup>†</sup> and Melanie S. Sanford<sup>\*,†</sup>

<sup>†</sup>Department of Chemistry, University of Michigan, 930 N. University Avenue, Ann Arbor, Michigan 48109, United States

<sup>‡</sup>School of Natural Sciences – Chemistry, University of Tasmania, Hobart, Tasmania 7001, Australia

**S** Supporting Information

**ABSTRACT:** The treatment of pyridine- and pyrazole-ligated Ni<sup>II</sup>  $\sigma$ -aryl complexes with Selectfluor results in C(sp<sup>2</sup>)–F bond formation under mild conditions. With appropriate design of supporting ligands, diamagnetic Ni<sup>IV</sup>  $\sigma$ -aryl fluoride intermediates can be detected spectroscopically and/or isolated during these transformations. These studies demonstrate for the first time that Ni<sup>IV</sup>  $\sigma$ -aryl fluoride complexes participate in challenging C(sp<sup>2</sup>)–F bond-forming reductive elimination to yield aryl fluoride products.



## INTRODUCTION

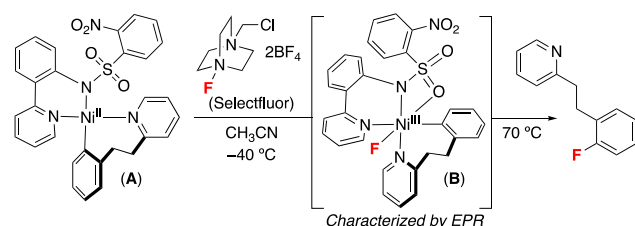
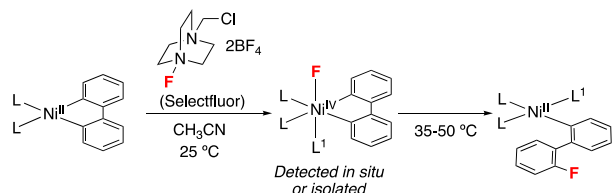
Over the past decade, there has been significant progress in the development of Pd-, Cu-, and Ag-mediated/catalyzed methods for the formation of aryl–fluoride bonds.<sup>1,2</sup> These protocols are finding increasing application in the synthesis of fluorine-containing pharmaceutical candidates<sup>3</sup> as well as <sup>18</sup>F-labeled radiotracers.<sup>4</sup> Given that C(sp<sup>2</sup>)–F bond formation is typically the most challenging step of these transformations,<sup>5</sup> fundamental studies of C(sp<sup>2</sup>)–F reductive elimination from transition metal  $\sigma$ -aryl fluoride complexes have been critical for the advancement of this field.<sup>2a,c,d,6–11</sup> For instance, organometallic investigations of C(sp<sup>2</sup>)–F coupling at Pt, Pd, Cu, and Ag complexes<sup>6a,2a,h,7b,8</sup> have guided the identification of ligand scaffolds that are most effective for promoting this transformation. Related studies have provided critical insights into the types of electrophilic fluorinating reagents that enable oxidatively induced C(sp<sup>2</sup>)–F bond formation at different metals.<sup>2g,6a,9,12</sup> Furthermore, stoichiometric studies have provided detailed information about factors impacting the selectivity of productive C(sp<sup>2</sup>)–F coupling versus competing side reactions such as carbon–heteroatom<sup>13</sup> and phosphorus–fluorine<sup>8c,d,14</sup> bond-forming pathways.

Moving forward, a key frontier for this field is to find new transition metals/oxidation states that participate in this challenging transformation, in order to further expand the scope and diversity of synthetic methods for C(sp<sup>2</sup>)–F bond formation. Nickel has been known to mediate the formation of C–F bonds under oxidative conditions since the introduction of the Simons process in the 1930s. This electrochemical fluorination method involves the use of plated anodes to access perfluorinated molecules.<sup>15</sup>

A more recent advance in the field of Ni-mediated fluorination came in a 2012 report by Ritter and co-workers demonstrating oxidatively induced aryl–F and aryl–<sup>18</sup>F coupling reactions of Ni<sup>II</sup>( $\sigma$ -aryl) complexes.<sup>16</sup> These transformations were proposed to proceed via high-valent Ni intermediates. However, the structures and oxidation states (Ni<sup>III</sup> versus Ni<sup>IV</sup>) of these species were not identified in the original report. More recently, Ritter has shown that the stoichiometric reaction of the Ni<sup>II</sup> model complex **A** with Selectfluor affords a transient Ni<sup>III</sup>(aryl)(F) species with proposed structure **B** (Figure 1A).<sup>17</sup> Intermediate **B** was detected *in situ* via EPR spectroscopy and shown to undergo C(sp<sup>2</sup>)–F coupling upon heating to 70 °C. These results implicate the feasibility of aryl–F bond formation from Ni<sup>III</sup> centers. However, key questions remain about what other classes of ligands and oxidation states of Ni enable this transformation.

Recent work from our group has shown that multidentate pyridine- and pyrazole-containing ligands support organometallic Ni<sup>III</sup> and Ni<sup>IV</sup> complexes that participate in challenging reductive elimination reactions, including C(sp<sup>3</sup>)–heteroatom and C(sp<sup>2</sup>)–CF<sub>3</sub> couplings.<sup>18–20</sup> We hypothesized that analogous ligand systems might enable the isolation and reactivity studies of high-valent Ni( $\sigma$ -aryl)(F) intermediates. We demonstrate herein that a variety of pyridine and pyrazole-ligated Ni<sup>II</sup> complexes participate in oxidatively induced C(sp<sup>2</sup>)–F bond formation upon treatment with Selectfluor. Furthermore, we show for the first time that several of these transformations proceed via

Received: June 28, 2019

A. Ritter (2017): Oxidatively-Induced C–F Coupling from Proposed Ni<sup>III</sup> IntermediateB. This Work: Oxidatively-Induced C–F Coupling from Isolable Ni<sup>IV</sup> Intermediates

**Figure 1.** Intermediates in oxidatively induced aryl–F coupling from organometallic Ni<sup>II</sup> complexes. (A) Ni<sup>III</sup> intermediate detected by Ritter. (B) This work (Ni<sup>IV</sup> intermediate detected and isolated).

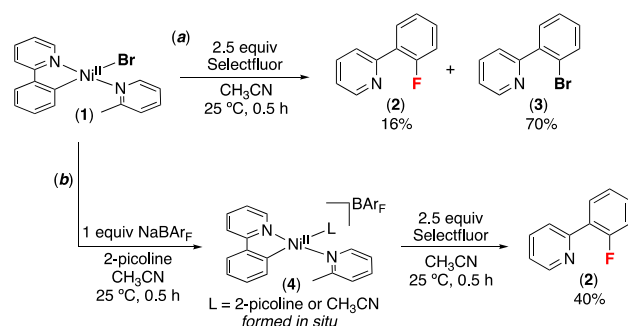
detectable and even isolable Ni<sup>IV</sup>  $\sigma$ -aryl fluoride intermediates (Figure 1B).

## RESULTS AND DISCUSSION

The Ni<sup>II</sup> complex **1** was selected as an initial model system for exploring oxidatively induced aryl–fluoride coupling at Ni. The pyridine donor ligands of **1** are similar to those employed in a variety of Ni-catalyzed carbon–heteroatom cross-coupling reactions.<sup>21</sup> Additionally, previous work from our group has demonstrated that the treatment of **1** with Cl<sup>+</sup> oxidants (e.g., PhICl<sub>2</sub>) results in C(sp<sup>2</sup>)–Cl and C(sp<sup>2</sup>)–Br bond formation to afford a mixture of 2-(2-chlorophenyl)pyridine (53%) and 2-(2-bromophenyl)pyridine (25%).<sup>22</sup> Based on these results, we hypothesized that F<sup>+</sup> oxidants might induce an analogous C(sp<sup>2</sup>)–F coupling reaction to generate **2**. Indeed, the reaction of **1** with Selectfluor for 0.5 h at 25 °C afforded **2** in modest (16%) yield (Scheme 1). However, the major product of this reaction was 2-(2-bromophenyl)pyridine (**3**, 70% yield), which is derived from competitive C(sp<sup>2</sup>)–Br bond formation.

We reasoned that the formation of the undesired aryl bromide product **3** could be minimized by abstraction of the bromide ligand from **1** prior to oxidation with Selectfluor. The treatment of **1** with 1 equiv of sodium tetrakis[3,5-bis(trifluoromethyl)phenyl]borate (NaBAR<sub>F</sub>) in the presence of 4 equiv of 2-picoline resulted in the precipitation of NaBr,

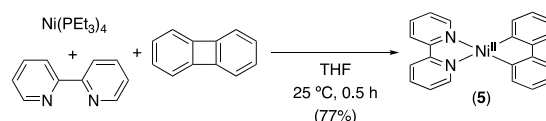
### Scheme 1. Oxidatively Induced Aryl–Fluoride Coupling from **1**



accompanied by the formation of the cationic Ni<sup>II</sup> complex **4**. As predicted, the subsequent *in situ* oxidation of this intermediate with Selectfluor resulted in a significantly improved ratio of **2** to **3** (40% and 23% yield, respectively) (Scheme 1b). This result demonstrates the feasibility of selective aryl–F coupling from Ni complexes supported by pyridine ligands.

The reactions in Scheme 1 proceed rapidly at room temperature, and no intermediates are detected by <sup>19</sup>F NMR or EPR spectroscopy. Thus, we next sought to design systems that would enable the detection and isolation of high-valent Ni intermediates in analogous transformations. Previous work has shown that organometallic Ni<sup>III</sup> and Ni<sup>IV</sup> complexes are stabilized by ligands that are rigid, multidentate, and strongly electron donating.<sup>13–15,23</sup> As such, we envisioned that Ni<sup>II</sup> precursor **5**, which contains bidentate bipyridine and biphenyl ligands, could allow for intermediates of this oxidatively induced fluorination to be observed at room temperature (Scheme 2).

### Scheme 2. Synthesis of Ni<sup>II</sup> Complex **5**



Complex **5** was prepared via the treatment of Ni(PEt<sub>3</sub>)<sub>4</sub> with biphenylene in the presence of 2,2'-bipyridine. The Ni<sup>II</sup> product was isolated in 77% yield as an analytically pure dark blue solid and was characterized by <sup>1</sup>H and <sup>13</sup>C NMR spectroscopy. X-ray quality crystals were obtained by recrystallization from a tetrahydrofuran/acetone solution of **5** at –35 °C, and an ORTEP diagram is shown in Figure 2. The most notable feature of this structure is the significant distortion from the square plane, with an angle of 24.2° between the N1–Ni–N2 and C11–Ni–C22 planes.

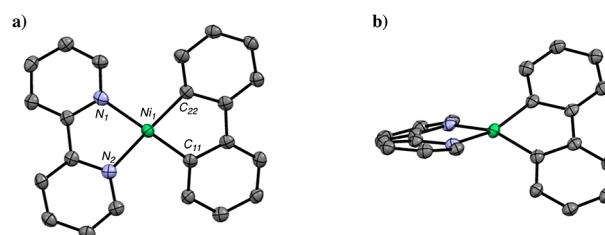
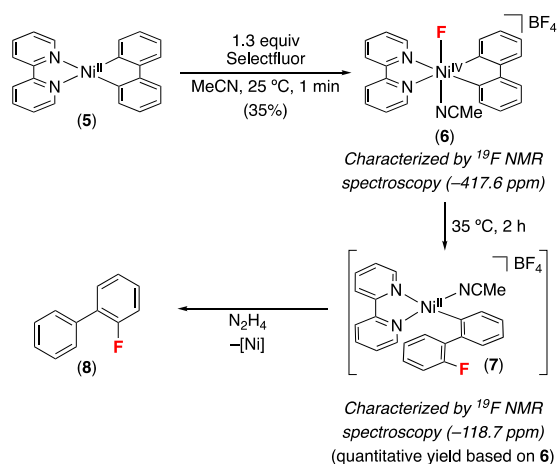


**Figure 2.** ORTEP diagram for complex **5**. Hydrogen atoms have been omitted for clarity; thermal ellipsoids are drawn at 50% probability. Bond lengths (Å): Ni1–N1 = 1.952, Ni1–N2 = 1.964, Ni1–C11 = 1.902, Ni1–C22 = 1.898. Bond angles (deg): N1–Ni1–N2 = 82.6, C11–Ni1–C22 = 83.8.

The treatment of **5** with 1.3 equiv of Selectfluor in MeCN at room temperature resulted in an immediate color change from purple to orange. This coincided with the appearance of a <sup>19</sup>F NMR resonance at –417.6 ppm, implicating the formation of a diamagnetic nickel fluoride intermediate.<sup>24</sup> <sup>1</sup>H NMR spectroscopic analysis of this species shows eight aromatic signals that each integrate to two protons (Figure S4). Furthermore, analysis of a solution of *in situ*-generated **6** by EPR spectroscopy did not show the presence of any paramagnetic species (Figure S11). These data along with the

observed reactivity of this complex (*vide infra*) implicate a symmetrical Ni<sup>IV</sup> cation with fluoride and solvent ligands at the axial positions (Scheme 3). The observation of this

### Scheme 3. Aryl–Fluoride Bond Formation from Putative Ni<sup>IV</sup> Intermediate (6)



putative Ni<sup>IV</sup> fluoride intermediate (6) stands in notable contrast to Ritter's oxidation of Ni<sup>II</sup> complex A with Selectfluor, which yielded a Ni<sup>III</sup>-fluoride (B, Figure 1a).

Heating an acetonitrile solution of *in situ*-generated 6 for 2 h at 35 °C resulted in the disappearance of the Ni–F resonance at -417.6 ppm and concomitant formation of an aryl–fluoride signal at -118.7 ppm in the <sup>19</sup>F NMR spectrum (Figure S8). This is consistent with C(sp<sup>2</sup>)–F bond-forming reductive elimination from 6 to afford the diamagnetic Ni<sup>III</sup> product 7. <sup>19</sup>F NMR spectroscopic monitoring of this reaction shows that the rate of consumption of 6 closely tracks that of the formation of this aryl fluoride product (Figure 3). Furthermore, the yield of this product is quantitative relative to the initial concentration of 6.

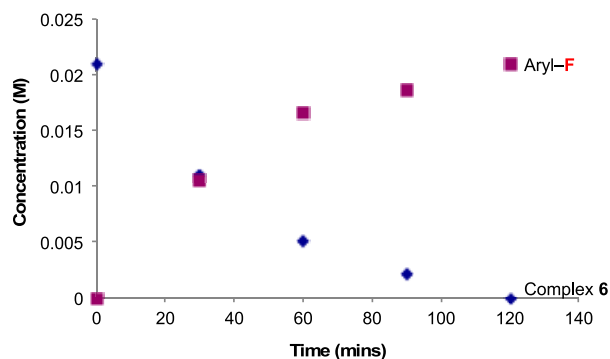


**Figure 3.** Reaction profile for C(sp<sup>2</sup>)–F bond formation from 6. Reaction was monitored by <sup>19</sup>F NMR spectroscopy using 4-fluoroanisole as an internal standard.

The proposed Ni<sup>III</sup> product 7 could not be isolated cleanly. As such, a reductive workup with hydrazine was performed to release the  $\sigma$ -aryl ligand from Ni, and both GC and NMR spectroscopic analysis of the isolated organic product confirmed the formation of aryl fluoride 8.<sup>25,26</sup> Overall, these experiments demonstrate the first example of C(sp<sup>2</sup>)–F coupling from a detectable Ni<sup>IV</sup>(aryl)(F) complex.

Further insight into the reactivity of 5 was obtained by conducting a computational analysis of the transformations depicted in Scheme 3.<sup>27</sup> Gaussian 09 was used at the B3LYP<sup>28</sup> level of density functional theory (DFT) for geometry optimization (see SI for complete details). These studies focused on intermediates that are expected to lead to the experimentally observed isomer of complex 6. On the basis of these calculations, an energetically plausible pathway for the formation of 6 is shown in Figure 4. It commences with the transfer of one electron from 5 to Selectfluor to generate A. Interaction of the organometallic product A with solvent (MeCN) affords the Ni<sup>III</sup> intermediate A-MeCN, which then receives the F atom from the reduced Selectfluor to form 6.<sup>29,30</sup> Conversion of 6 to other isomers is precluded by the low barrier for reductive elimination (see Figure S24 for details). Overall, the favorability of each step within the oxidation pathway depicted in Figure 4 shows the competence of Selectfluor as an oxidant for accessing Ni<sup>IV</sup> species from Ni<sup>II</sup> precursors.

We also evaluated the possibility that complex 6 might exist as a Ni<sup>III</sup> species that is antiferromagnetically coupled to a ligand-centered radical. However, all attempts to optimize for a structure containing two unpaired electrons of opposite spin by DFT were unsuccessful, either directly or via an attempted triplet state exhibiting expulsion of MeCN from the coordination sphere. In contrast, the proposed diamagnetic Ni<sup>IV</sup> structure for complex 6 underwent facile optimization.

We next calculated a pathway for reductive elimination from complex 6, resulting in an overall reaction profile (Figure 5) consistent with the experimentally observed process in Scheme 3. Both dissociative and concerted mechanisms were considered (see SI for complete details), revealing a preference for a concerted mechanism that proceeds through a single transition state (TS-6/7) with  $\Delta G^\ddagger = 9.3$  kcal/mol to afford reductive elimination product 7. This low barrier is consistent with experimental observations that *in situ* generated 6 undergoes C(sp<sup>2</sup>)–F bond formation under mild conditions (2 h at 35 °C).

These calculations motivated us to seek experimental evidence in support of the single-electron transfer mechanism for the oxidation of 5 with Selectfluor. The addition of 1 equiv of TEMPO to this oxidation reaction completely inhibited formation of complex 6 (Figure S6). These results, in addition to the well-precedented one-electron reactivity of Selectfluor, are consistent with a pathway like that depicted in Figure 4.<sup>31</sup>

A final set of studies focused on designing a Ni<sup>IV</sup>(aryl)-(fluoride) complex that could be isolated and fully characterized. Our previous work has shown that replacing the neutral bidentate 2,2'-bipyridyl ligand with the anionic tridentate tris(pyrazolyl)borate (Tp) ligand dramatically enhances the stability of high-valent Ni complexes.<sup>18</sup> As such, we reacted the anionic TpNi<sup>II</sup> complex 9 with Selectfluor in MeCN. Within 30 min at 25 °C this transformation afforded the Ni<sup>IV</sup>–F complex 10, which was isolated in 48% yield (Scheme 4).

Complex 10 was characterized via <sup>1</sup>H, <sup>19</sup>F, and <sup>11</sup>B NMR spectroscopy. In addition, X-ray quality crystals of 10 were obtained via recrystallization from MeCN at -35 °C, and the solid-state structure is shown in Figure 6. Overall, these data are all consistent with a diamagnetic octahedral Ni<sup>IV</sup>–fluoride structure in both solution and the solid state.

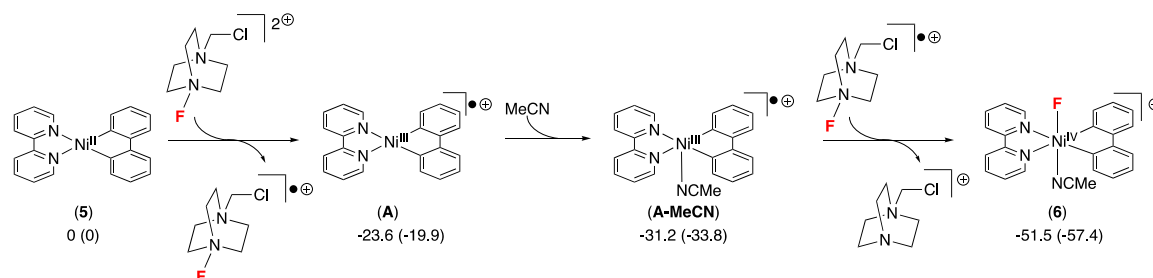


**Figure 4.** Relative energies of intermediates in the SET pathway for reaction of 5 with Selectfluor to afford 6. Energies  $\Delta G$  ( $\Delta H$ ) are in kcal/mol relative to 5.

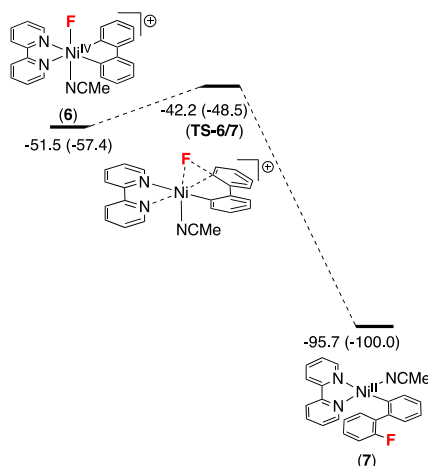


**Figure 5.** Energy profile for C(sp<sup>2</sup>)-F bond formation from 6. Energies  $\Delta G$  ( $\Delta H$ ) in kcal/mol relative to 5.

#### Scheme 4. Synthesis of (Tp)Ni<sup>IV</sup>(C<sub>6</sub>H<sub>4</sub>-*o*-C<sub>6</sub>H<sub>4</sub>)(F) (10)

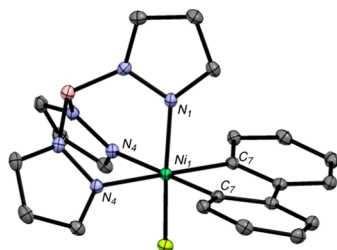
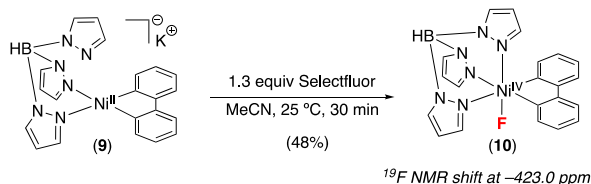
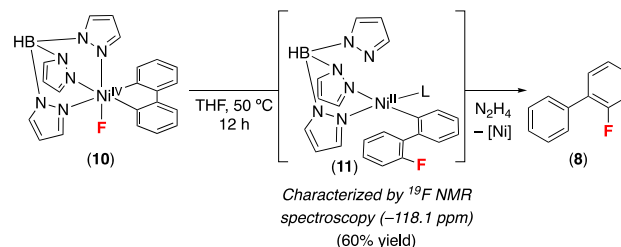


**Figure 6.** ORTEP diagram for complex 10. Hydrogen atoms have been omitted for clarity; thermal ellipsoids are drawn at 50% probability. Bond lengths (Å): Ni1-N1 = 1.888, Ni1-N4 = 2.031, Ni1-C7 = 1.952. Bond angles (deg): N4-Ni1-N4 = 84.9, C7-Ni1-C7 = 84.0.

Complex 10 is stable at -35 °C for several hours in MeCN. However, heating a MeCN solution of 10 at 50 °C for 12 h results in complete consumption of this Ni<sup>IV</sup> species and the formation of an aryl fluoride product in 10% yield as determined by <sup>19</sup>F NMR spectroscopy ( $\delta$  -118.1 ppm, Figure S13). Previous investigations of aryl-oxygen coupling from similar Ni<sup>IV</sup> complexes revealed that reductive

elimination yields could be improved by conducting this reaction in ethereal solvents.<sup>32</sup> Similarly, the yield of the aryl-fluoride product increased to 60% by changing the solvent from MeCN to tetrahydrofuran (THF). We hypothesize that this aryl fluoride product is the Ni<sup>II</sup>- $\sigma$ -aryl complex 11 (Scheme 5); however, this species proved

#### Scheme 5. Aryl-Fluoride Bond Formation from (Tp)Ni<sup>IV</sup>(C<sub>6</sub>H<sub>4</sub>-*o*-C<sub>6</sub>H<sub>4</sub>)(F) (10)



challenging to isolate cleanly. As such, a reductive workup with hydrazine was performed to release the  $\sigma$ -aryl ligand from Ni, and GC analysis confirmed the identity of the organic product as aryl fluoride 8. Overall, these studies of complex 10 represent the first demonstration of C(sp<sup>2</sup>)-F coupling from an isolated Ni<sup>IV</sup> complex.

We next used DFT to interrogate whether reductive elimination from complex 10 proceeds via a concerted or dissociative mechanism. Figure 7 illustrates the energy profiles for these two different pathways. The barriers for C(sp<sup>2</sup>)-F bond-forming reductive elimination in this system range from approximately 20 to 23 kcal/mol, consistent with the much slower rate of reductive elimination from 10 compared to that from the bipyridine complex 6. These calculations show a relatively small 3.2 kcal/mol preference for the concerted pathway (via TS<sub>10/IV</sub>) compared to the dissociative pathway (via TS<sub>I/II</sub>).

## SUMMARY AND CONCLUSIONS

In conclusion, this article demonstrates that the treatment of a variety of nitrogen-ligated  $\sigma$ -aryl Ni<sup>II</sup> complexes with Selectfluor results in C(sp<sup>2</sup>)-F coupling. In several of these systems, diamagnetic Ni<sup>IV</sup>  $\sigma$ -aryl fluoride intermediates were detected and/or isolated. These results demonstrate the viability of C(sp<sup>2</sup>)-F bond-forming reductive elimination from Ni<sup>IV</sup> complexes under mild conditions. In addition, they stand in interesting contrast to Ni<sup>III</sup>-mediated fluorination reactions demonstrated by Ritter. Future work will focus on leveraging these results to develop Ni<sup>II/IV</sup>-catalyzed fluorination reactions.

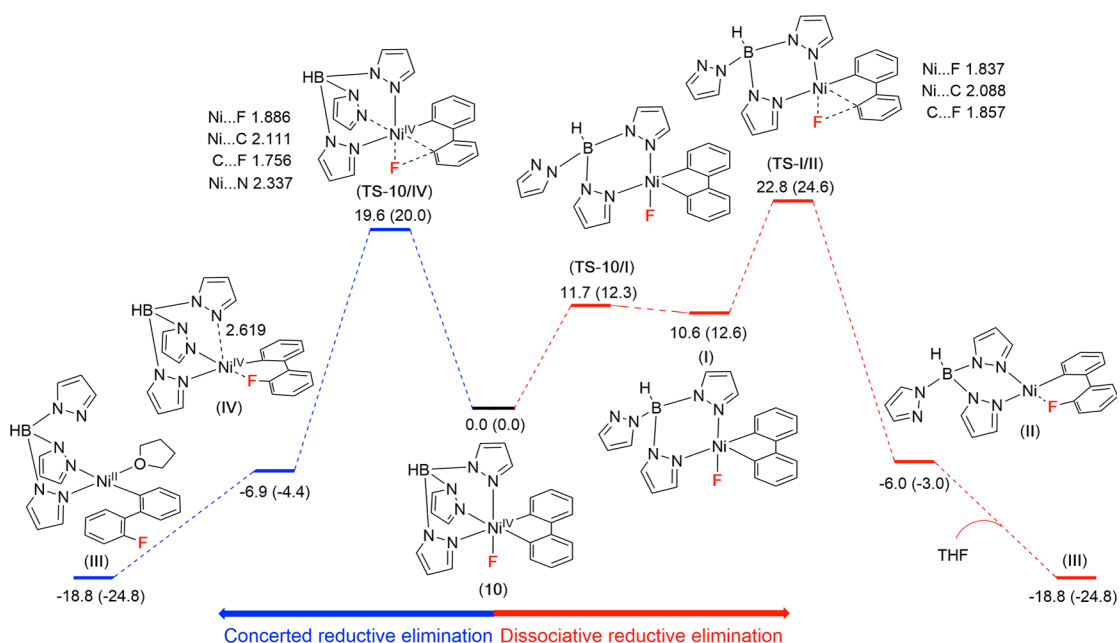


**Figure 7.** Energy profile for the reductive elimination steps from complex 10. Complex I also forms an adduct with solvent THF, at  $\Delta G$  ( $\Delta H$ ) 9.0 (0.6) kcal/mol. Energies  $\Delta G$  ( $\Delta H$ ) are in kcal/mol.

## ■ ASSOCIATED CONTENT

### Supporting Information

The Supporting Information is available free of charge on the ACS Publications website at DOI: 10.1021/jacs.9b06896.

Crystallographic data (CIF)

3D chemical structure (XYZ)

Experimental details, optimization tables, and complete characterization data for all new compounds (PDF)

## ■ AUTHOR INFORMATION

### Corresponding Author

\*mssanfor@umich.edu

### ORCID

Allan J. Canty: 0000-0003-4091-6040

Melanie S. Sanford: 0000-0001-9342-9436

### Notes

The authors declare no competing financial interest.

## ■ ACKNOWLEDGMENTS

This work was supported by the National Science Foundation Grant CHE-1111563, the Australian Research Council, and the Australian National Computing Infrastructure. E.A.M. thanks Rackham Graduate School (RMF) and the NSF for graduate fellowships. We gratefully acknowledge funding from NSF Grant CHE-0840456 for X-ray instrumentation.

## ■ REFERENCES

- Select reviews: (a) Furuya, A. S.; Kamlet, A. S.; Ritter, T. Catalysis for Fluorination and Trifluoromethylation. *Nature* **2011**, *473*, 470–477. (b) Campbell, M. G.; Ritter, T. Modern Carbon-Fluorine Bond Forming Reactions for Aryl Fluoride Synthesis. *Chem. Rev.* **2015**, *115*, 612–633. (c) Sather, A. C.; Buchwald, S. L. The Evolution of Pd<sup>0</sup>/Pd<sup>II</sup>-Catalyzed Aromatic Fluorination. *Acc. Chem. Res.* **2016**, *49*, 2146–2157.
- For examples of metal-mediated/catalyzed arene fluorination methods, see: (a) Watson, D. A.; Su, M.; Teverovskiy, G.; Zhang, Y.; Fortanet-García, J.; Kinzel, T.; Buchwald, S. L. Formation of ArF

from LPdAr(F): Catalytic Conversion of Aryl Triflates to Aryl Fluorides. *Science* **2009**, *325*, 1661–1664. (b) Furuya, T.; Strom, A. E.; Ritter, T. Silver-Mediated Fluorination of Functionalized Aryl Stannanes. *J. Am. Chem. Soc.* **2009**, *131*, 1662–1663. (c) Wang, X.; Mei, T.-S.; Yu, J.-Q. Versatile Pd(OTf)<sub>2</sub> > 2H<sub>2</sub>O-Catalyzed *Ortho*-Fluorination Using NMP as a Promoter. *J. Am. Chem. Soc.* **2009**, *131*, 7520–7521. (d) Tang, P.; Furuya, T.; Ritter, T. Silver-Catalyzed Late-Stage Fluorination. *J. Am. Chem. Soc.* **2010**, *132*, 12150–12154. (e) Fier, P. S.; Hartwig, J. F. Copper-Mediated Fluorination of Aryl Iodides. *J. Am. Chem. Soc.* **2012**, *134*, 10795–10798. (f) Cochrane, N. A.; Nguyen, H.; Gagne, M. R. Catalytic Enantioselective Cyclization and C3-Fluorination of Polyenes. *J. Am. Chem. Soc.* **2013**, *135*, 628–631. (g) Fier, P. S.; Luo, J.; Hartwig, J. F. Copper-Mediated Fluorination of Arylboronate Esters. Identification of a Copper(III) Fluoride Complex. *J. Am. Chem. Soc.* **2013**, *135*, 2552–2559. (h) Truong, T.; Klimovica, K.; Daugulis, O. Copper-Catalyzed, Directing Group-Assisted Fluorination of Arene and Heteroarene C-H Bonds. *J. Am. Chem. Soc.* **2013**, *135*, 9342–9345. (i) Talbot, E. P. A.; Fernandes, T.; de, A.; McKenna, J. M.; Toste, F. D. Asymmetric Palladium-Catalyzed Directed Intermolecular Fluoroarylation of Styrenes. *J. Am. Chem. Soc.* **2014**, *136*, 4101–4104. (j) Mu, X.; Zhang, H.; Chen, P.; Liu, G. Copper-Catalyzed Fluorination of 2-Pyridyl Aryl Bromides. *Chem. Sci.* **2014**, *5*, 275–280. (k) Zhang, Q.; Yin, X.-S.; Chen, K.; Zhang, S.-Q.; Shi, B.-F. Stereoselective Synthesis of Chiral  $\beta$ -Fluoro and  $\alpha$ -Amino Acids via Pd(II)-Catalyzed Fluorination of Unactivated Methylene C(sp<sup>3</sup>)-H Bonds: Scope and Mechanistic Studies. *J. Am. Chem. Soc.* **2015**, *137*, 8219–8226. (l) Lou, S.-J.; Chen, Q.; Wang, Y.-F.; Xu, D.-Q.; Du, X.-H.; He, J.-Q.; Mao, Y.-J.; Xu, Z.-Y. Selective C-H Bond Fluorination of Phenols with a Removable Directing Group: Late-Stage Fluorination of 2-Phenoxy Nicotinate Derivatives. *ACS Catal.* **2015**, *5*, 2846–2849. (m) Chen, X.-Y.; Sorensen, E. J. Pd-Catalyzed, *ortho* C-H Methylation and Fluorination of Benzaldehydes Using Orthanilic Acids as Transient Directing Groups. *J. Am. Chem. Soc.* **2018**, *140*, 2789–2792. (n) Mao, Y.-J.; Lou, S.-J.; Hao, H.-Y.; Xu, D.-Q. Selective C(sp<sup>3</sup>)-H and C(sp<sup>2</sup>)-H Fluorination of Alcohols Using Practical Auxiliaries. *Angew. Chem., Int. Ed.* **2018**, *57*, 14085–14089.

(3) Zhou, Y.; Wang, J.; Gu, Z.; Wang, S.; Zhu, W.; Aceña, J. L.; Soloshonok, V. A.; Izawa, K.; Liu, H. Next Generation of Fluorine-Containing Pharmaceuticals, Compounds Currently in Phase II-III

Trials of Major Pharmaceutical Companies: New Structural Trends and Therapeutic Areas. *Chem. Rev.* **2016**, *116*, 422–518.

(4) Preshlock, S.; Tredwell, M.; Gouverneur, V. <sup>18</sup>F-Labeling of Arenes and Heteroarenes for Applications in Positron Emission Tomography. *Chem. Rev.* **2016**, *116*, 719–766.

(5) Grushin, V. V. The Organometallic Fluorine Chemistry of Palladium and Rhodium: Studies toward Aromatic Fluorination. *Acc. Chem. Res.* **2010**, *43*, 160–171.

(6) (a) Ball, N. D.; Sanford, M. S. Synthesis and Reactivity of a Mono- $\sigma$ -Aryl Palladium(IV) Fluoride Complex. *J. Am. Chem. Soc.* **2009**, *131*, 3796–3797. (b) Hickman, A. J.; Sanford, M. S. High-Valent Organometallic Copper and Palladium in Catalysis. *Nature* **2012**, *484*, 177–185.

(7) For examples of fundamental studies conducted by Buchwald, see: (a) Maimone, T. J.; Milner, P. J.; Kinzel, T.; Zhang, Y.; Takase, M. K.; Buchwald, S. L. Evidence for In Situ Catalyst Modification During the Pd-Catalyzed Conversion of Aryl Triflates to Aryl Fluorides. *J. Am. Chem. Soc.* **2011**, *133*, 18106–18109. (b) Sather, A. C.; Lee, H. G.; De La Rosa, V. Y.; Yang, Y.; Müller, P.; Buchwald, S. L. A Fluorinated Ligand Enables Room-Temperature and Regioselective Pd-Catalyzed Fluorination of Aryl Triflates and Bromides. *J. Am. Chem. Soc.* **2015**, *137*, 13433–13438.

(8) For examples of fundamental studies conducted by Grushin, see: (a) Fraser, S. L.; Antipin, M. Y.; Khroustalyov, V. N.; Grushin, V. V. Molecular Fluoro Palladium Complexes. *J. Am. Chem. Soc.* **1997**, *119*, 4769–4770. (b) Pilon, M. C.; Grushin, V. V. Synthesis and Characterization of Organopalladium Complexes Containing a Fluoro Ligand. *Organometallics* **1998**, *17*, 1774–1781. (c) Grushin, V. V. Thermal Stability, Decomposition Paths, and Ph/Ph Exchange Reactions of  $[(\text{Ph}_3\text{P})_2\text{Pd}(\text{Ph})\text{X}]$  (X = I, Br, Cl, F, and HF<sub>2</sub>). *Organometallics* **2000**, *19*, 1888–1900. (d) Grushin, V. V.; Marshall, W. J. Ar-F Reductive Elimination from Palladium(II) Revisited. *Organometallics* **2007**, *26*, 4997–5002.

(9) For select examples of fundamental studies by Ritter, see: (a) Furuya, T.; Benitez, D.; Tkatchouk, E.; Strom, A. E.; Tang, P.; Goddard, W. A.; Ritter, T. Mechanism of C-F Reductive Elimination from Palladium(IV) Fluorides. *J. Am. Chem. Soc.* **2010**, *132*, 3793–3807. (b) Brandt, J. R.; Lee, E.; Boursalian, G. B.; Ritter, T. Mechanism of Electrophilic Fluorination with Pd(IV): Fluoride Capture and Subsequent Oxidative Fluoride Transfer. *Chem. Sci.* **2014**, *5*, 169–179.

(10) For fundamental studies by Ribas, see: (a) Casitas, A.; Canta, M.; Solà, M.; Costas, M.; Ribas, X. Nucleophilic Aryl Fluorination and Aryl Halide Exchange Mediated by a Cu<sup>I</sup>/Cu<sup>III</sup> Catalytic Cycle. *J. Am. Chem. Soc.* **2011**, *133*, 19386–19392. (b) Font, M.; Acuna-Pares, F.; Parella, T.; Serra, J.; Luis, J.; Luis, J. M.; Lloret-Fillol, J.; Costas, M.; Ribas, X. Direct Observation of Two-Electron Ag(I)/Ag(III) Redox Cycles in Coupling Catalysis. *Nat. Commun.* **2014**, *5*, 4373–4382.

(11) For fundamental studies of Pt-mediated fluorination, see: (a) Zhao, S.-B.; Wang, R.-Y.; Nguyen, H.; Becker, J. J.; Gagné, M. R. Electrophilic Fluorination of Cationic Pt-Aryl Complexes. *Chem. Commun.* **2012**, *48*, 443–445. (b) Dubinsky-Davidchik, I.; Goldberg, I.; Vigalok, A.; Vedernikov, A. N. Selective Aryl-Fluoride Reductive Elimination from a Platinum(IV) Complex. *Angew. Chem., Int. Ed.* **2015**, *54*, 12447–12541.

(12) Lee, E.; Kamlet, A. S.; Powers, D. C.; Neumann, C. N.; Boursalian, G. B.; Furuya, T.; Choi, D. C.; Hooker, J. M.; Ritter, T. A Fluoride-Derived Electrophilic Late-Stage Fluorination Reagent for PET Imaging. *Science* **2011**, *334*, 639–642.

(13) Camasso, N. M.; Pérez-Temprano, M. H.; Sanford, M. S. C(sp<sup>3</sup>)-O Bond-Forming Reductive Elimination from Pd<sup>IV</sup> with Diverse Oxygen Nucleophiles. *J. Am. Chem. Soc.* **2014**, *136*, 12771–12775.

(14) Marshall, W. J.; Grushin, V. V. Palladium(II) and Palladium(0) Complexes of BINAP(O) (2-(Diphenylphosphino)-2'-diphenylphosphinyl)-1,1'-binaphthyl). *Organometallics* **2003**, *22*, 555–562.

(15) (a) Fuchigami, T. In *Electrochemistry in the Preparation of Fluorine and its Components*; Ves Childs, W., Ed.; The Electrochemical Society: NJ, 1997; Vol. 97-15; pp 1–12. (b) Sartori, P.; Ignat-Ev, N. The Actual State of Our Knowledge about Mechanism of Electrochemical Fluorination in Anhydrous Hydrogen Fluoride (Simons Process). *J. Fluorine Chem.* **1998**, *87*, 157–162. (c) Ignat-Ev, N. V.; Willner, H.; Sartori, P. Electrochemical Fluorination (Simons Process) - A Powerful Tool for the Preparation of New Conducting Salts, Ionic liquids, and Strong Bronsted acids. *J. Fluorine Chem.* **2009**, *130*, 1183–1191.

(16) Lee, E.; Hooker, J. M.; Ritter, T. Nickel-Mediated Oxidative Fluorination for PET with Aqueous [<sup>18</sup>F] Fluoride. *J. Am. Chem. Soc.* **2012**, *134*, 17456–17458.

(17) Lee, H.; Börgel, J.; Ritter, T. Carbon-Fluorine Reductive Elimination from Nickel(III) Complexes. *Angew. Chem., Int. Ed.* **2017**, *56*, 6966–6969.

(18) Camasso, N. M.; Sanford, M. S. Design, Synthesis, and Carbon-Heteroatom Coupling Reactions of Organometallic Nickel(IV) Complexes. *Science* **2015**, *347*, 1218–1220.

(19) Bour, J. R.; Camasso, N. M.; Sanford, M. S. Oxidation of Ni(II) to Ni(IV) with Aryl Electrophiles Enables Ni-Mediated Aryl-CF<sub>3</sub> Coupling. *J. Am. Chem. Soc.* **2015**, *137*, 8034–8037.

(20) Bour, J. R.; Camasso, N. M.; Meucci, E. A.; Kampf, J. W.; Canty, A. J.; Sanford, M. S. Carbon-Carbon Bond-Forming Reductive Elimination from Isolated Nickel(III) Complexes. *J. Am. Chem. Soc.* **2016**, *138*, 16105–16111.

(21) For select examples, see: (a) Omar-Amrani, R.; Thomas, A.; Brenner, E.; Schneider, R.; Fort, Y. Efficient Nickel-Mediated Intramolecular Amination of Aryl Chlorides. *Org. Lett.* **2003**, *5*, 2311–2314. (b) Zhang, C.-P.; Vivic, D. A. Nickel-Catalyzed Synthesis of Aryl Trifluoromethyl Sulfides at Room Temperature. *J. Am. Chem. Soc.* **2012**, *134*, 183–185. (c) Serrano, E.; Martin, R. Nickel-Catalyzed Reductive Amidation of Unactivated Alkyl Bromides. *Angew. Chem., Int. Ed.* **2016**, *55*, 11207–11211. (d) Han, J.-B.; Dong, T.; Vivic, D. A.; Zhang, C.-P. Nickel-Catalyzed Trifluoromethylselenolation of Aryl Halides Using the Readily Available [Me<sub>4</sub>N][SeCF<sub>3</sub>] Salt. *Org. Lett.* **2017**, *19*, 3919–3922.

(22) Higgs, A. T.; Zinn, P. J.; Simmons, S. J.; Sanford, M. S. Oxidatively Induced Carbon-Halogen Bond-Forming Reactions at Nickel. *Organometallics* **2009**, *28*, 6142–6144.

(23) For select examples of high-valent Ni complexes supported by these types of ligands, see: (a) Pandarus, V.; Zargarian, D. New Pincer-Type Diphosphinito (POCOP) Complexes of Ni<sup>II</sup> and Ni<sup>III</sup>. *Chem. Commun.* **2007**, 978–980. (b) Martinez, G. E.; Ocampo, C.; Park, Y. J.; Fout, A. R. Accessing Pincer Bis(carbene) Ni(IV) Complexes from Ni(II) via Halogen and Halogen Surrogates. *J. Am. Chem. Soc.* **2016**, *138*, 4290–4293. (c) Schultz, J. W.; Fuchigami, K.; Zheng, B.; Rath, N. P.; Mirica, L. M. Isolated Organometallic Nickel(III) and Nickel(IV) Complexes Relevant to Carbon-Carbon Bond Formation Reactions. *J. Am. Chem. Soc.* **2016**, *138*, 12928–12934.

(24) For examples of Ni<sup>IV</sup>-F complexes with similar <sup>19</sup>F NMR signals, see: (a) D'Accrisio, F.; Borja, P.; Saffon-Merceron, N.; Fustier-Boutignon, M.; Mézailles, N.; Nebra, N. C-H Bond Trifluoromethylation of Arenes Enabled by a Robust, High-Valent Nickel(IV) Complex. *Angew. Chem., Int. Ed.* **2017**, *56*, 12898–12902. (b) Chong, E.; Kampf, J. W.; Ariafor, A.; Canty, A. J.; Sanford, M. S. Oxidatively Induced C-H Activation at High Valent Nickel. *J. Am. Chem. Soc.* **2017**, *139*, 6058–6061. (c) Kosobokov, M. D.; Sandleben, A.; Vogt, N.; Klein, A.; Vivic, D. A. Nitrogen-Nitrogen Bond Formation via a Substrate-Bound Anion at a Mononuclear Nickel Platform. *Organometallics* **2018**, *37*, 521–525.

(25) This was further confirmed by treating the crude product with trifluoroacetic acid. Again, aryl fluoride **8** was formed based on GC and GCMS analysis.

(26) For use of hydrazine in a similar reductive workup, see: Aguilera, E. Y.; Sanford, M. S. Model Complexes for the Palladium-

Catalyzed Transannular C-H Functionalization of Alicyclic Amines. *Organometallics* **2019**, *38*, 138–142.

(27) Frisch, M. J.; Trucks, G. W.; Schlegel, H. B.; Scuseria, G. E.; Robb, M. A.; Cheeseman, J. R.; Scalmani, G.; Barone, V.; Mennucci, B.; Petersson, G. A.; Nakatsuji, H.; Caricato, M.; Li, X.; Hratchian, H. P.; Izmaylov, A. F.; Bloino, J.; Zheng, G.; Sonnenberg, J. L.; Hada, M.; Ehara, M.; Toyota, K.; Fukuda, R.; Hasegawa, J.; Ishida, M.; Nakajima, T.; Honda, Y.; Kitao, O.; Nakai, H.; Vreven, T.; Montgomery, J. A., Jr.; Peralta, J. E.; Ogliaro, F.; Bearpark, M.; Heyd, J. J.; Brothers, E.; Kudin, K. N.; Staroverov, V. N.; Kobayashi, R.; Normand, J.; Raghavachari, K.; Rendell, A.; Burant, J. C.; Iyengar, S. S.; Tomasi, J.; Cossi, M.; Rega, N.; Millam, J. M.; Klene, M.; Knox, J. E.; Cross, J. B.; Bakken, V.; Adamo, C.; Jaramillo, J.; Gomperts, R.; Stratmann, R. E.; Yazyev, O.; Austin, A. J.; Cammi, R.; Pomelli, C.; Ochterski, J. W.; Martin, R. L.; Morokuma, K.; Zakrzewski, V. G.; Voth, G. A.; Salvador, P.; Dannenberg, J. J.; Dapprich, S.; Daniels, A. D.; Farkas, O.; Foresman, J. B.; Ortiz, J. V.; Cioslowski, J.; Fox, D. J. *Gaussian 09*, revision A.02; Gaussian, Inc.: Wallingford, CT, 2009.

(28) Lee, C. T.; Yang, W. T.; Parr, R. G. Development of the Colle-Salvetti Correlation-Energy Formula into a Functional of the Electron Density. *Phys. Rev. B: Condens. Matter Mater. Phys.* **1988**, *37*, 785–789. (b) Miehlich, B.; Savin, A.; Stoll, H.; Preuss, H. Results Obtained with the Correlation Energy Density Functionals of Becke and Lee, Yang and Parr. *Chem. Phys. Lett.* **1989**, *157*, 200–206. (c) Becke, A. D. Density-Functional Thermochemistry. III. The Role of Exact Exchange. *J. Chem. Phys.* **1993**, *98*, 5648–5652.

(29) A similar pathway has recently been reported for the formation of Ni<sup>IV</sup>-R products from Ni<sup>III</sup> intermediates: Bour, J. R.; Ferguson, D. M.; McClain, E. J.; Kampf, J. W.; Sanford, M. S. Connecting Organometallic Ni(III) and Ni(IV): Reactions of Carbon-Centered Radicals with High-Valent Organonickel Complexes. *J. Am. Chem. Soc.* **2019**, *141*, 8914–8920.

(30) Another plausible mechanism involves a stepwise sequence of two single-electron oxidations involving initial F<sup>•</sup> transfer to **5** followed by 1e<sup>-</sup> transfer (Scheme S20). A third pathway involving a concerted 2e<sup>-</sup> F<sup>+</sup> transfer to **5** (Scheme S21), for which a closed-shell configuration allows facile DFT access to a transition state and IRC analysis, is inconsistent with experimental evidence for a SET process.

(31) (a) Banks, R. E.; Lawrence, N. J.; Popplewell, A. L. Oxidation of Benzylic Alcohols and Benzaldehydes with Selectfluor Reagent F-TEDA-BF<sub>4</sub> [1-chloromethyl-4-(1,4-diazoniabicyclo[2.2.2]octane bis-(tetrafluoroborate))]. *Synlett* **1994**, *1994*, 831. (b) Umemoto, T.; Fukami, S.; Tomizawa, G.; Harasawa, K.; Kawada, K.; Tomita, K. Power- and Structure-Variable Fluorinating Agents. The N-Fluoropyridinium Salt System. *J. Am. Chem. Soc.* **1990**, *112*, 8563–8575. (c) Bockman, T. M.; Lee, K. Y.; Kochi, J. K. Time-Resolved Spectroscopy and Charge-Transfer Photochemistry of Aromatic EDA Complexes with X-Pyridinium Cations. *J. Chem. Soc., Perkin Trans. 2* **1992**, *2*, 1581–1594. (d) Piana, S.; Devillers, I.; Togni, A.; Rothlisberger, U. The Mechanism of Catalytic Enantioselective Fluorination: Computational and Experimental Studies. *Angew. Chem., Int. Ed.* **2002**, *41*, 979–982. (e) Geng, C.; Du, L.; Liu, F.; Zhu, R.; Liu, C. Theoretical Study on the Mechanism of Selective Fluorination of Aromatic Compounds with Selectfluor. *RSC Adv.* **2015**, *5*, 33385–33391. (f) Ventre, S.; Petronijevic, F. R.; MacMillan, D. W. C. Decarboxylative Fluorination of Aliphatic Carboxylic Acids via Photoredox Catalysis. *J. Am. Chem. Soc.* **2015**, *137*, 5654–5657. (g) Rueda-Becerril, M.; Mahe, O.; Drouin, M.; Majewski, M. B.; West, J. G.; Wolf, M. O.; Sammis, G. M.; Paquin, J.-F. Direct C-F Bond Formation Using Photoredox Catalysis. *J. Am. Chem. Soc.* **2014**, *136*, 2637–2641. (h) Danahy, K. E.; Cooper, J. C.; Van Humbeck, J. F. Benzylic Fluorination of Aza-Heterocycles Induced by Single-Electron Transfer to Selectfluor. *Angew. Chem., Int. Ed.* **2018**, *57*, 5134–5138.

(32) Meucci, E. A.; Camasso, N. M.; Sanford, M. S. An Organometallic Ni(IV) Complex that Participates in Competing

Transmetalation and C(sp<sup>2</sup>)-O Bond-Forming Reductive Elimination Reactions. *Organometallics* **2017**, *36*, 247–250.